SPECTRUM OF THE NEAR INFRARED AIRGLOW AT THE MIDDLE LATITUDE

V.V. Bakanas (*Obukhov Institute of Atmospheric Physics, Russian Academy of Sciences, Pyzhevskii per. 3, Moscow, 119017 Russia, sem@mxo6.nifhi.ac.ru*)

Abstract. Registrograms of nightglow spectra in the wavelength interval 620–1050 nm, first obtained in absolute units (Rayleighs) for specific heliogeophysical conditions, are presented. They can serve as a modern atlas of the emission spectrum of the upper atmosphere. For any other given heliogeophysical conditions, spectrum parameters can be computed based on existing empirical models of the emissions of the upper atmosphere.

Introduction

The spectra of the nighttime upper atmosphere of the Earth in the wavelength interval 600–1050 nm have been recorded for several decades, and the obtained results of various form and quality are presented in [Krassovsky, 1950; Meinel, 1950; Krassovsky et al., 1962; Boadfoot and Kendall, 1968; Vlasyuk and Spiridonova, 1993; Osterbrock et al., 1996, 1997]. All the papers characterize only the spectral structure of the nightglow and bear no information about the energy parameters of the spectrum. This prevents the determination of the emission intensities within the given wavelength interval under different heliogeophysical conditions. In this paper, we are the first to present the results of the measurements of the spectral distribution of various emissions in the upper atmosphere for specific heliogeophysical conditions in absolute photometric units, Rayleighs, which is defined in [Barbier, 1963].

Measurement technique

An essential problem in recording the airglow of the upper atmosphere is its low intensity (several photons/cm^2 s). Therefore, from the outset of the studies, it was necessary to use high-transmission spectrographs and high-sensitivity detectors. Thus, the exposures of several tens of hours had to be used in the first attempts to record the airglow of the upper atmosphere using prism spectrographs and photographic technique. The specially designed high-transmission diffraction spectrographs SP-48, SP-49, and SP-50 [Gerasimova and Yakovleva, 1956; Katalog, 1959], combined with modern astronomical films [Dokuchaeva, 1994], made it possible to reduce the exposures to several hours. Combining photographic films with image tubes [Shcheglov, 1963; Zaidel' and Kurenkov, 1976], which are used to enhance the brightness of the recorded spectra [Potapov et al., 1978], marked an important advance in the detection of the weak airglow of the upper atmosphere. As a result, the times of emission recording in the visible and near infrared spectral region was several minutes to several tens of minutes. In addition to image tubes, the photoelectric measurement techniques with the use of photoelectric multipliers [Broadfoot and Kendall, 1968] were also applied.

The most important advantage of the photographic technique is that it allows one to record simultaneously the entire chosen spectral interval. In this case, the spectral distribution of the recorded emission is not distorted by either eventual variations in the atmospheric transparency or natural airglow fluctuations. Unfortunately, the photographic recording technique has a shortcoming: the processing of photographic materials is a complex and labor-consuming task, and nonlinear transformations are needed to convert photographic film densities into the intensities of the emissions that have caused these densities. In this sense, the photoelectric technique has an evident advantage, because it allows one to detect emissions in the form of electric signals, whose values are proportional to the emission intensity and are easily available for further automatic processing. However, this technique requires sequential scanning in front of the photomultiplier of the chosen spectral interval. Recording the weak airglow of the upper atmosphere requires that the scanning be slow enough to ensure the necessary signal integration, which can, as noted above, significantly distort the resulting spectral distribution of the emission measured.

In recent years, CCD detectors have come into wide use as a means of recording and analyzing faint emissions [Osterbrock et al., 1996, 1997]. These devices, which combine the advantages of both photographic and photoelectric techniques, have significantly expanded the possibilities for analyzing the parameters of the airglow of the upper atmosphere.

Since 1955, the temperature regime and structural and dynamic parameters of the upper atmospheric layers have been studied on the basis of the atmospheric airglow at the Zvenigorod research station (55.7 N, 36.8 E) of the Obukhov Institute of Atmospheric Physics, Russian Academy of Sciences. Atmospheric emissions were recorded using both photographic techniques, including those involving image-tube detectors, and photoelectric methods. Based on photographic records of the airglow of the upper atmosphere, a popular atlas of nightglow spectra [Krassovsky et al., 1962] was compiled in 1962 and it contains photographs and spectrograms of the emissions in the 300–1240 nm wavelength interval. However, registrograms of spectra are given in the units of photographic density. Moreover, the atlas by Krassovsky et al. [1962] provides examples of spectrograms for separate wavelength intervals obtained with 6-to 10-h exposures

at different times of the winter season, and, therefore, these spectra do not correspond to the same heliogeophysical conditions.
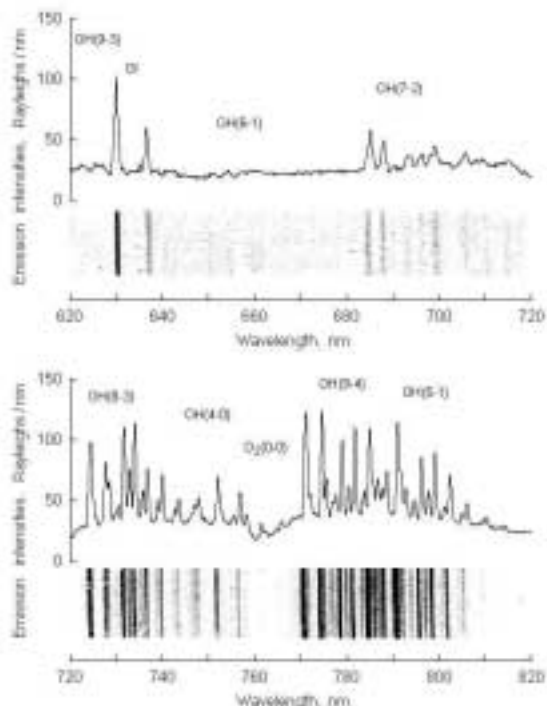

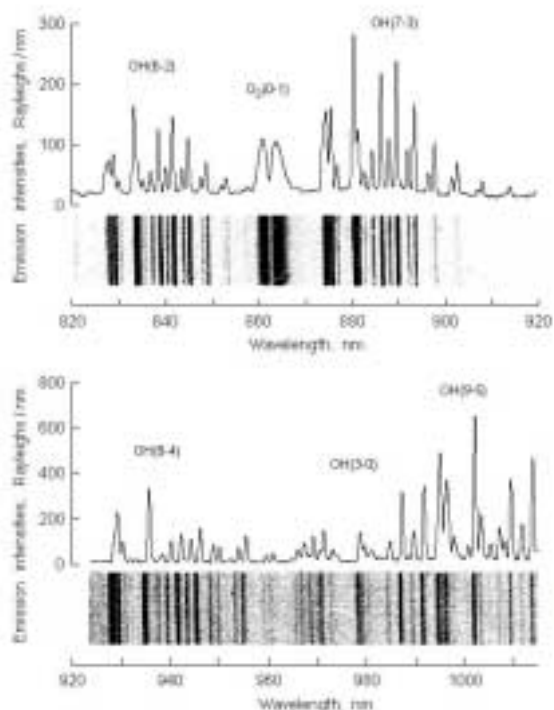**Fig. 1**. Spectrum of the upper atmosphere nightglow in the wavelength interval 620–820 nm.

Fig. 2. Spectrum of the upper atmosphere nightglow in the wavelength interval 820–1020 nm.
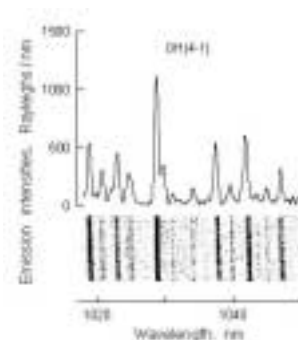

Fig. 3. Spectrum of the upper atmosphere nightglow in the wavelength interval 1020–1050 nm.

At present, the spectra of the airglow of the upper atmosphere at Zvenigorod station are recorded using a set of spectroscopic instruments [Gerasimova and Yakovleva, 1956; Catalogue, 1959] with INSTASPEC IV detectors [The Book..., 1999] equipped with 1024 x 128 and 1024 x 256 CCD-matrices with 26 x 26 μn pixels. To improve the signal-to-noise ratio, CCDs are cooled down to –40°C by a thermoelectric cooler. An interface board connects the detector to a PC used to automatically control the receiver operation during the registration of spectra and to perform photometric treatment.

We performed a regular absolute spectral calibration of the instrument using a standard lamp. The absolute calibration of the lamp itself was based, in turn, on the emission spectrum of the G8 III star Capella αAur, α = $5^h 15^m$, δ = 45°58', magnitude 0.03^m) [Kharitonov et al., 1972].

Results of measurements

Spectroscopic observations at the Zvenigorod station were made during clear weather at a zenith angle of 53° and azimuth of 157.4° counted from the southern direction. In this case, the geographic coordinates of the observed region at the height of 90 km were 56.7° N and 36.2° E.

Figures 1–3 show the picture example spectra with the 0.4-nm resolution, obtained in the wavelength interval 620–1050 nm and the corresponding registrograms. The spectra were obtained on September 19, 2000, with a 10-min exposure (0008– 0018 LT). This day corresponded to the solar and geomagnetic activity levels of $F_{[10.7]}$ = 207 and Kp = 3, respectively. The registrograms in all the spectral intervals have been corrected for the spectral sensitivity of the instrument. The spectral distribution of the observed emission intensities has been reduced to the zenith and is given in Rayleigh/nm. This distribution is caused by the emission of molecular hydroxyl $X^2\Pi$ (vibrational–rotational bands of the sequences Δv = 3, 4, 5), molecular oxygen ($b^1\Sigma^+_g$–$X^3\Sigma^?_g$) (Atmospheric band (0-1) 864.5 nm), the continuum (result of the NO + O photochemical process), and atomic oxygen (O(^{1}D) 630.0–636.4 nm). Artificial sources of light can to a certain degree

Table 1. Emission intensities in the upper atmosphere in the wavelength interval 620–1050 nm.

Wavelength, nm	Atmospheric gas component	Line	Emission intensities, Rayleighs
630.0	O(^{1}D)		80
636.4	O(^{1}D)		28
683.0	OH(X$^2\Pi$)	R (7,2)	41
686.7	OH(X$^2\Pi$)	Q	24
689.0	OH(X$^2\Pi$)	P2(2)	4
690.1	OH(X$^2\Pi$)	P1(2)	16
691.3	OH(X$^2\Pi$)	P2(3)	12
692.3	OH(X$^2\Pi$)	P1(3)	23
694.9	OH(X$^2\Pi$)	P1(4)	8
724.0	OH(X$^2\Pi$)	R (8,3)	75
728.0	OH(X$^2\Pi$)	Q	62
730.4	OH(X$^2\Pi$)	P2(2)	9
731.6	OH(X$^2\Pi$)	P1(2)	53
732.9	OH(X$^2\Pi$)	P2(3)	16
734.1	OH(X$^2\Pi$)	P1(3)	47
735.8	OH(X$^2\Pi$)	P2(4)	11
736.9	OH(X$^2\Pi$)	P1(4)	23
739.1	OH(X$^2\Pi$)	P2(5)	6
740.1	OH(X$^2\Pi$)	P1(5)	16
748.0	OH(X$^2\Pi$)	R (4,0)	35
752.8	OH(X$^2\Pi$)	Q	34
755.8	OH(X$^2\Pi$)	P2(2)	4
757.2	OH(X$^2\Pi$)	P1(2)	18
758.6	OH(X$^2\Pi$)	P2(3)	5
772.0	OH(X$^2\Pi$)	R (9,4)	88
775.0	OH(X$^2\Pi$)	Q	53
778.0	OH(X$^2\Pi$)	P2(2)	11
779.4	OH(X$^2\Pi$)	P1(2)	37
781.0	OH(X$^2\Pi$)	P2(3)	12
782.1	OH(X$^2\Pi$)	P1(3)	43
784.0	OH(X$^2\Pi$)	P2(4)	10
787.0	OH(X$^2\Pi$)	R (5,1)	130*
791.4	OH(X$^2\Pi$)	Q	72
795.0	OH(X$^2\Pi$)	P2(2)	10
796.5	OH(X$^2\Pi$)	P1(2)	32
798.0	OH(X$^2\Pi$)	P2(3)	13
799.4	OH(X$^2\Pi$)	P1(3)	36
801.5	OH(X$^2\Pi$)	P2(4)	8
802.7	OH(X$^2\Pi$)	P1(4)	26
805.3	OH(X$^2\Pi$)	P2(5)	5
806.2	OH(X$^2\Pi$)	P1(5)	12
805.8	OH(X$^2\Pi$)	P(6)	5
829.0	OH(X$^2\Pi$)	R (6,2)	130
835.0	OH(X$^2\Pi$)	Q	150
838.3	OH(X$^2\Pi$)	P2(2)	24
839.9	OH(X$^2\Pi$)	P1(2)	70
841.6	OH(X$^2\Pi$)	P2(3)	25
843.1	OH(X$^2\Pi$)	P1(3)	81
845.3	OH(X$^2\Pi$)	P2(4)	22
846.5	OH(X$^2\Pi$)	P1(4)	61
849.4	OH(X$^2\Pi$)	P2(5)	17
850.5	OH(X$^2\Pi$)	P1(5)	35
849.4	OH(X$^2\Pi$)	P2(6)	7
854.9	OH(X$^2\Pi$)	P1(6)	16
865.4	O$_2$(b$^1\Sigma^+_g$)	R,P(0,1)	420
877.1	OH(X$^2\Pi$)	R (7,3)	280
883.0	OH(X$^2\Pi$)	Q	240
886.8	OH(X$^2\Pi$)	P2(2)	44
888.5	OH(X$^2\Pi$)	P1(2)	120
890.3	OH(X$^2\Pi$)	P2(3)	52
891.9	OH(X$^2\Pi$)	P1(3)	130
894.3	OH(X$^2\Pi$)	P2(4)	40
895.8	OH(X$^2\Pi$)	P1(4)	90
898.8	OH(X$^2\Pi$)	P2(5)	19
900.0	OH(X$^2\Pi$)	P1(5)	49
903.8	OH(X$^2\Pi$)	P2(6)	16
904.9	OH(X$^2\Pi$)	P1(6)	35
909.3	OH(X$^2\Pi$)	P2(7)	6
910.4	OH(X$^2\Pi$)	P1(7)	15
915.6	OH(X$^2\Pi$)	P(8)	11
931.5	OH(X$^2\Pi$)	R (8,4)	300
937.8	OH(X$^2\Pi$)	Q	210
942.0	OH(X$^2\Pi$)	P2(2)	67
943.9	OH(X$^2\Pi$)	P1(2)	89
945.8	OH(X$^2\Pi$)	P2(3)	67
947.6	OH(X$^2\Pi$)	P1(3)	97
950.2	OH(X$^2\Pi$)	P2(4)	54
951.9	OH(X$^2\Pi$)	P1(4)	12
955.2	OH(X$^2\Pi$)	P2(5)	38
956.5	OH(X$^2\Pi$)	P1(5)	76
960.7	OH(X$^2\Pi$)	P2(6)	22
961.9	OH(X$^2\Pi$)	P1(6)	29
967.1	OH(X$^2\Pi$)	R (3,0)	400
979.5	OH(X$^2\Pi$)	Q	130
984.9	OH(X$^2\Pi$)	P2(2)	58
987.2	OH(X$^2\Pi$)	P1(2)	200
989.5	OH(X$^2\Pi$)	P2(3)	92
991.5	OH(X$^2\Pi$)	P1(3)	220
995.9	OH(X$^2\Pi$)	R (9,5)	910**
1001.2	OH(X$^2\Pi$)	Q	470
1002.3	OH(X$^2\Pi$)	Q	150
1003.9	OH(X$^2\Pi$)	Q	50
1006.1	OH(X$^2\Pi$)	P2(2)	100
1008.2	OH(X$^2\Pi$)	P1(2)	250
1010.3	OH(X$^2\Pi$)	P2(3)	120
1012.3	OH(X$^2\Pi$)	P1(3)	330
1018.9	OH(X$^2\Pi$)	R (4,1)	1670***
1029.1	OH(X$^2\Pi$)	Q	1240
1034.8	OH(X$^2\Pi$)	P2(2)	180
1037.3	OH(X$^2\Pi$)	P1(2)	520
1039.7	OH(X$^2\Pi$)	P2(3)	220
1041.9	OH(X$^2\Pi$)	P1(3)	560
1045.1	OH(X$^2\Pi$)	P2(4)	170
1047.0	OH(X$^2\Pi$)	P1(4)	380

Notes:
   * Intensities of the P1(4), P2(5), and P1(5) lines of the (9-4) band included.
  ** Intensities of the P2(4) and P1(4) lines of the (3-0) band included.
 *** Intensities of the P2(4), P1(4), P2(5), and P1(5) lines of the (9-5) band included.

contribute to the continuum due to their emission scattering in the atmosphere. Note that many OH emission bands are distorted by absorption bands of molecular oxygen and water vapor. Table 1 gives the emission intensities of the molecular and atomic lines considered. These data can be easily converted into energy units using the following formula:

$$I \, (erg/(cm^2 \, sr \, s)) = 1.58 \, 10^{-10} \, I \, (Rayleigh)/\lambda \, (nm).$$

Table 2 gives the total emission intensities of the hydroxyl bands. We determined them for a rotational temperature of 216 K inferred from the OH (6–2) band using a method described by Shefov [1961]. We estimated the total band emission intensities in accordance with Piterskaya and Shefov [1975] based on this rotational temperature and the first lines of the Q and P branches. The error in measuring absolute emission rates of the lines considered was 6%, and the relative error was 1%. The latter makes it possible to determine the rotational temperature with an accuracy of 3 K.

Table 2. Hydroxyl band emission intensities.

Band	Emission intensities, Rayleighs
3-0	1140±70
4-0	180±20
4-1	3740±230
5-1	300±20
6-2	680±40
7-2	120±10
7-3	880±50
8-3	360±30
8-4	590±40
9-4	470±30
9-5	3220±200

Conclusion

The spectral distribution of the intensity of the airglow of the upper atmosphere presented in this paper in absolute units (Rayleighs) for the wavelength interval 620–1050 nm with a spectral resolution of 0.4 nm is a modern version of the atlas of the nightglow in the midlatitude upper atmosphere. The chief value of the spectra presented here is that they allow the absolute intensity to be easily estimated within narrow wavelength intervals. This makes it possible to eliminate background nightglow, caused mainly by

hydroxyl emission within the given spectral region in order to identify faint extra-atmospheric sources. Moreover, these data make it possible to obtain absolute estimates of the parameters of various emissions of the upper atmosphere and those of the atmosphere itself with the help of the empirical models [Semenov and Shefov 1996, 1997a,b,c] of the variations in the parameters of emissions within different wavelength intervals, which take into account different regular and quasi-regular variations (long-term trend, modulation that depends on the 11-year solar-activity cycle, 5.5-year and quasi-biennial, latitude, seasonal, diurnal, and lunar variations). This, in turn, makes it possible to analyze the behavior of the temperature regime and dynamical and structural parameters of the middle and upper atmosphere in situations when the data for particular emissions can be obtained.

References

Osterbrock D.E., Fulbright J.P., Bida T.A., Night-Sky High-Resolution Spectral Atlas of OH and O2 Emission Lines for Echelle Spectrograph Wavelength Calibration. II. Publ. Astron. Soc. Pac., Vol. 109, № 735, Pp. 614–627, 1997.

Gerasimova N.G., Yakovleva A.V., A Set of High-transmission Grating Spectrographs, Prib. Tekh. Eksp., № 1, Pp. 83–86, 1956.

Krassovsky V.I., Shefov N.N., Yarin V.I., Atlas of the Airglow Spectrum λ=3000–12 400 A, Planet. Space Sci., Vol. 9, № 12, Pp. 883–915, 1962.

The Book of Photon Tools. Stratford: Oriel Instruments, 1999.

Piterskaya N.A., Shefov N.N., An Intensity Distribution in the OH Rotational–Vibrational Bands, (Aurorae and Nightglow), Krassovskii, V.I., Ed., Moscow: Nauka, № 23, Pp. 69–122, 1975.

Semenov A.I., Shefov N.N., An Empirical Model for Variations in the Hydroxyl Emission, Geomagn. Aeron., Vol. 36, № 4, Pp. 468–480, 1996.